Antiferromagnetism in CuO studied by neutron polarimetry

1991 J. Phys.: Condens. Matter 3 4281

(http://iopscience.iop.org/0953-8984/3/23/016)

J. Phys.: Condens. Matter 3 (1991) 4281–4287. Printed in the UK

Antiferromagnetism in CuO studied by neutron polarimetry

P J Brown†, T Chattopadhyay†‡, J B Forsyth§, V Nunez†‖ and F Tasset†

† Institut Laue–Langevin, 156X, 38042 Grenoble Cédex, France
‡ Centre d'Etudes Nucleaires, 85X, 38041 Grenoble Cédex, France
§ Rutherford Appleton Laboratory, Chilton, Oxon OX11 0QX, UK
‖ Department of Physics, King's College London, Strand, London WC2R 2LS, UK

Received 15 March 1991

Abstract. Single-crystal neutron diffraction measurements on cupric oxide, CuO, using a zero-field neutron polarimeter have confirmed that the Cu^{2+} moments are parallel to the monoclinic $\boldsymbol{b}$ axis in the commensurate antiferromagnetic phase stable below 213 K. Any component of moment in the $\boldsymbol{a}$–$\boldsymbol{c}$ plane must have a magnitude less than 0.03 of the total. The incommensurate antiferromagnetic phase, stable between 213 K and the Néel temperature of 230 K, has a propagation vector (0.506, 0, −0.483) as previously reported, but the elliptical envelope of the helical modulation at 215.5 K is shown to have its axes parallel to [010] and in the $\boldsymbol{a}$–$\boldsymbol{c}$ plane making an angle of 28.2(8)° to [001] in β obtuse. The envelope is almost circular with the ratio of the $\boldsymbol{b}$ to $\boldsymbol{a}$–$\boldsymbol{c}$ components of 1.03(1) and the plane of the moments makes an angle of 73.0(5)° to the propagation vector. The new magnetic model produces an equally good fit to the original unpolarized neutron diffraction intensities as the previous model, in which the Cu^{2+} moments were confined to the $\boldsymbol{a}$–$\boldsymbol{c}$ plane with a more elliptical envelope, and gives a root mean square Cu^{2+} effective moment of 0.27(1) μ_B.

1. Introduction

The continuing interest in the role of nominally divalent copper coordinated by oxygen in the formation of high-T_c superconductors has led to a number of studies of cupric oxide CuO itself. Pure CuO provides an opportunity to study the magnetic properties of Cu^{2+} square-planar coordinated by oxygen in a relatively simple system: a complete understanding of the magnetic properties of CuO may indicate whether magnetic mechanisms actually play any role in the hole-pairing in high-temperature superconductors. CuO orders magnetically at $T_N = 230$ K to an incommensurate spiral phase with a wave vector $\boldsymbol{k} = (0.506, 0, -0.483)$ which is temperature independent within the experimental resolution (Forsyth *et al* 1988). At $T_L = 213$ K this incommensurate phase locks into a commensurate phase with the wave vector $\boldsymbol{k} = (\frac{1}{2}, 0, -\frac{1}{2})$. Low temperature unpolarized neutron single crystal intensity data gave a good fit to an antiferromagnetic structure in which the Cu^{2+} moments of 0.65(3) μ_B lay parallel and antiparallel to the monoclinic $\boldsymbol{b}$ axis ($a = 4.684$, $b = 3.423$, $c = 5.129$ Å, $\beta = 99.54°$). Above T_L, the even weaker magnetic intensities were better fitted by a model in which the moments lay in the $\boldsymbol{a}$–$\boldsymbol{c}$ plane than by one in which they were amplitude modulated and aligned parallel to [010]

Some further improvement in the agreement was obtained by allowing the moments to follow an elliptical envelope with its major axis corresponding to 0.38(2) μ_B directed 33(2)° to c in β obtuse. However, no exhaustive search for alternatives to these two basic structures was made.

Since the original study was carried out, Yablonskii (1990) has sought to derive the magnetic structures through a study of the exchange paths and two further neutron studies have been reported. In the first of these, Yang *et al* (1988) found essentially the same structure for the low temperature, commensurate phase but did not mention the transition at 213 K. Subsequently, the same group confirmed the existence of the incommensurate phase from single crystal measurements, but found two satellites displaced equally by $\pm(0.0125, 0, 0.0125)$ about the positions of the magnetic reflections in the commensurate phase (Yang *et al* 1989). In view of this continuing interest in the magnetism of CuO and related compounds and some conflicting experimental data, it was decided to verify the propagation vector of the incommensurate phase and to use a generalised neutron polarization analysis technique to provide more direct evidence for the moment directions in the two antiferromagnetic phases of CuO. The relation between the input polarization $\boldsymbol{P}$ and the output polarization $\boldsymbol{P}_0$ for a purely magnetic reflection is a special case of the general expression given by Blume (1963):

$$\boldsymbol{P}_0 \mathrm{I} = \boldsymbol{P}(-\boldsymbol{Q}\cdot\boldsymbol{Q}^*) + 2\mathrm{Re}(\boldsymbol{P}\cdot\boldsymbol{Q})\boldsymbol{Q}^* - \mathrm{Im}(\boldsymbol{Q}\times\boldsymbol{Q}^*)$$

where $\mathrm{I} = \boldsymbol{Q}\cdot\boldsymbol{Q}^* + \mathrm{Im}(\boldsymbol{P}\cdot[\boldsymbol{Q}\times\boldsymbol{Q}^*])$, $\boldsymbol{Q}$ is the generalized magnetic interaction vector and $\boldsymbol{Q}^*$ its complex conjugate. The first two terms act on the input polarization $\boldsymbol{P}$ to rotate it about $\boldsymbol{Q}$ and the last term can create polarization if $\boldsymbol{Q}$ is complex. In particular, a single domain sample of a simple helimagnet will create polarization parallel or antiparallel to the scattering vectors of its magnetic reflections.

We now report the results of this work which confirms the original model of Forsyth *et al* (1988) for the commensurate phase but calls for a modification of the moment directions in their incommensurate structure.

2. The experiment

The large, 130 mg single crystal used in the experiment was grown by Wanklyn and Garrard (1983) at the Clarendon Laboratory, Oxford University, by flux growth in a platinum crucible. The starting materials for the flux were MoO_3, V_2O_3 and K_2CO_3. The sample was first examined by conventional unpolarized neutron diffraction and shown to order at $T_N = 230(1)$ K to the incommensurate phase in which a single magnetic reflection is displaced from the position of each magnetic reflection in the commensurate phase. The wave vector $\boldsymbol{k}$ was also in agreement with the original single crystal neutron diffraction data of Forsyth *et al* (1988), namely $\boldsymbol{k} = (-0.506, 0, 0.483)$. The incommensurate phase was again shown to lock into a commensurate phase with $\boldsymbol{k} = (\frac{1}{2}, 0, -\frac{1}{2})$ at $T_L = 213.0(5)$ K. The crystal was then carefully aligned and mounted with its [010] axis vertical in the zero-field polarimeter CRYOPAD on the IN20 polarized beam triple axis spectrometer at the Institut Laue Langevin, Grenoble. This crystal orientation was chosen so that the propagation vectors of both magnetic phases lay in the horizontal plane of the analyser and detector motion.

The principles and operation of the CRYOPAD have been fully described elsewhere by Tasset (1989) and Brown *et al* (1990). In short, it allows both the input neutron beam polarization to be set to any desired angle and the magnitude and direction of the

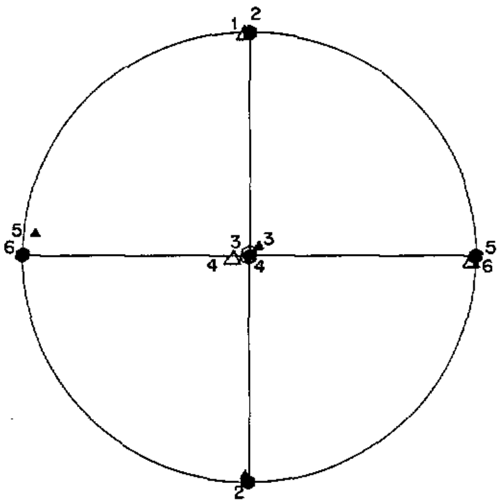

Figure 1. Stereographic projection of the incident and scattered polarization directions for the ($\frac{1}{2}$ 0 $-\frac{1}{2}$) reflection from the commensurate magnetic structure of CuO at 100 K. The incident directions are marked by hexagons and the scattered directions by triangles, the filled symbols mark poles in the upper and open symbols those in the lower hemisphere. The number associated with each symbol is the sequence number in the scan and can be used to identify corresponding incident and scattered directions. The outgoing polarizations were: 1, 0.877; 2, 0.878; 3, 0.891; 4, 0.865; 5, 0.880 and 6, 0.881.

polarization in a diffracted beam to be found under the control of a PDP11/73 computer. The diffracting sample is kept in a field-free region and its temperature can be maintained in the range 1.5–315 K. The Heusler alloy monochromator and analyser crystals of IN20 were set to a wavelength of 1.532 Å. Although the CRYOPAD makes it possible to set the input polarization $\boldsymbol{P}$ to any desired angle, it is convenient from the point of view of subsequent analysis to make scans in which $\boldsymbol{P}$ is varied in the three principal planes defined by the axes X parallel to the scattering vector $\boldsymbol{\kappa}$, Z vertical and Y making the right-handed set. In view of the weak scattered intensity and the time available, the present measurements were restricted to the six 'cardinal directions' parallel to $\pm X$, $\pm Y$ and $\pm Z$.

2.1. The commensurate phase at 100 K

Figure 1 shows a stereographic projection of the six cardinal input polarizations and the location of the corresponding output polarizations for the ($\frac{1}{2}$ 0 $-\frac{1}{2}$) reflection. A vertically polarized input beam is scattered without change in direction, whereas input polarizations along the X or Y directions are completely reversed in the scattered beam. These observations immediately show that the magnetic moments on the Cu atoms are aligned parallel and antiparallel to the vertical Z axis which is [010]. Similar observations were made for the reflections ($-\frac{1}{2}$ 0 $\frac{1}{2}$), ($-\frac{3}{2}$ 0 $\frac{3}{2}$) and ($\frac{3}{2}$ 0 $\frac{1}{2}$). All these measurements serve to set a limit on the magnitude of any component of moment which could be present in the $\boldsymbol{a}$–$\boldsymbol{c}$ plane and this is estimated to be 0.03 of the total moment of 0.65(3) μ_B (Forsyth *et al* 1988).

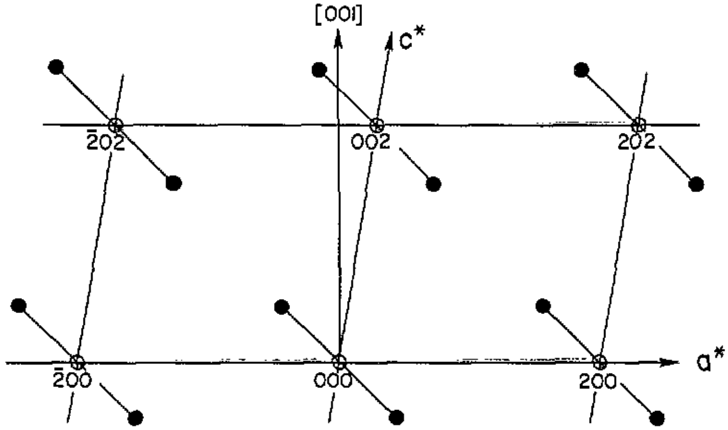

Figure 2. A (010) section of reciprocal lattice of CuO showing the location of the low $\boldsymbol{\kappa}$ magnetic satellites.

2.2. The incommensurate phase at 215.5 K

Figure 2 illustrates the location of the low $\boldsymbol{\kappa}$ magnetic satellites which occur in the $\boldsymbol{a}^*$–$\boldsymbol{c}^*$ plane of reciprocal space. The fundamental reflection (0.506, 0, −0.483) was reasonably strong with a peak count rate of some 250 cps, but the remainder were relatively weak with count rates in the range 2–10 cps. Long counting times were required to locate the direction of the scattered polarization in the weaker reflections, especially in cases where the polarization was low, when six hours were needed for each of the cardinal directions. The reflections were first located with the input polarization vertical and the analysing direction set parallel: the peak reflected intensity was then found by scanning the crystal about the vertical axis and summing the counts for flipped and unflipped output polarizations at each position. One feature of these results was immediately obvious; in some reflections the ratio of flipped to unflipped neutrons was close to unity whereas for others it was larger and in one case (0.506, 0, 1.517) it was over 10 and corresponded to the input beam polarization of 0.87. In this latter case it is clear that the only component of any modulated magnetic moment to enter $\boldsymbol{Q}$ must also be vertical. This conclusion is supported by the full series of six measurements shown in figure 3(a); in each case, no beam depolarization occurs and the results are analogous to those obtained for the magnetic reflections of the commensurate phase. Figure 3(b), however, illustrates the very different behaviour of the fundamental reflection (−0.506, 0, 0.483): in this case the output polarization is low, ~10%, and rotation towards X for incident polarization along Y or Z, but it is again its maximum but reversed for $\boldsymbol{P}$ parallel or antiparallel to X, the scattering vector $\boldsymbol{\kappa}$. The average scattered intensity is approximately the same in all cases and these observations may be understood if, for this reflection, there is a component of $\boldsymbol{Q}$ which is perpendicular to [010]. The ratio of the amplitudes of the two components of moment and the orientation of the component lying in the a–c plane have been determined from the turn angles observed when $\boldsymbol{P}$ is along $\pm Y$ and $\pm Z$ for seven magnetic ($h0l$) reflections. The small changes in the amplitude of $\boldsymbol{P}_0$ as $\boldsymbol{P}$ is varied from X to $-X$ gives a direct indication that the domains of different chirality are unequally populated. Table 1 gives the results of the best least squares fit to all the observations (χ^2 4.2) which is given by a model in which the moment component along $\boldsymbol{b}$ is 1.03(1)

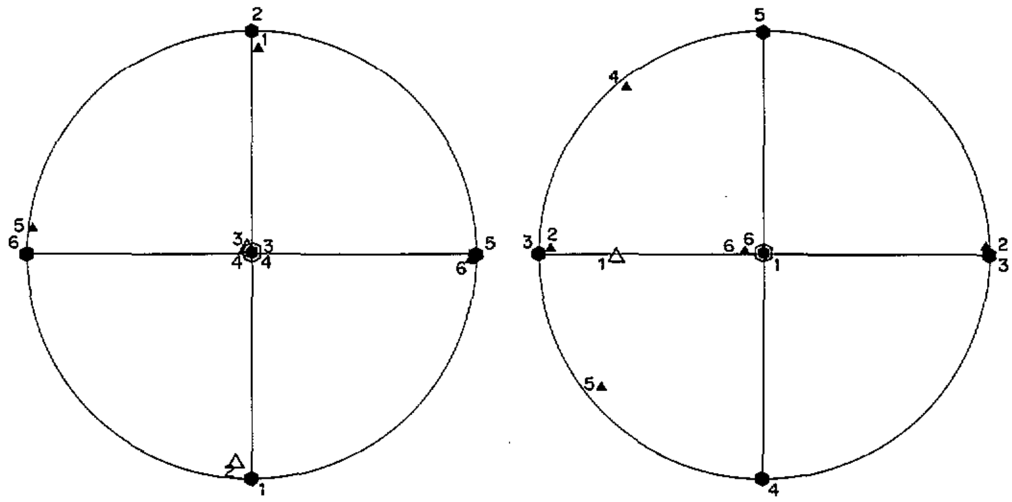

Figure 3. Stereographic projection of the incident and scattered polarization directions for (a) the (0.516, 0, 1.517) and (b) the (−0.516, 0, 0.483) satellite reflections from the incommensurate magnetic structure of CuO at 212.5 K. The labelling convention is as for figure 1 and the scattered polarizations are listed in table 1.

times the moment component in the ***a***–***c*** plane. The latter component makes an angle to [001] of 28.2(8)° in β obtuse and the domain ratio is 0.486(2): 0.514(2).

It is apparent from table 1 that the output polarization for the $\pm X$ directions of ***P*** is significantly reduced for the last four reflections as compared to the first three. This reduction cannot be accounted for by our model and we believe that it probably arises from a significant unpolarized background count rate which would affect the measured polarization more severely in these weaker reflections. In future experiments we shall attempt to correct for any such contribution by subtracting the count rates measured with the crystal rotated in omega from the reflecting position. In the absence of such data, we prefer to accept the estimated errors in the parameters obtained from the least squares fit to the raw data, since these are already small, rather than to include some empirical correction.

3. Conclusions

Zero-field neutron polarimetry can provide a very sensitive test for the correctness of magnetic structure models derived from unpolarized neutron integrated intensity measurements. In the present case its use has confirmed the original model for the commensurate phase of CuO first proposed by Forsyth *et al* (1988). Their proposed structure for the incommensurate phase has, however, been shown to be incorrect in as much as the moment envelope does not lie in the ***a***–***c*** plane, though its axis in this plane makes an angle of 28.2(8)° to ***c*** in β obtuse compared to the angle of 33(2)° obtained by Forsyth *et al*.

A re-analysis of the original unpolarized data on the basis of the new moment orientations and the ratio of the ***b*** to ***a***–***c*** moments produced only small improvements

Table 1. Least squares fit to the measured components of output polarization given by a model in which the moment along b is 1.03(1) times the moment in the a–c plane which makes an angle to [001] in β obtuse of 28.2(8)°.

h	k	l	P(in) x	P(in) y	P(in) z	Pout(obs) x	Pout(obs) y	Pout(obs) z	Pout(calc) x	Pout(calc) y	Pout(calc) z	Pout(diff) x	Pout(diff) y	Pout(diff) z
0.51	0.00	−0.48	0.001	−0.840	−0.004	−0.062	0.075	0.004	0.011	0.066	0.000	−0.073	0.008	0.004
			−0.001	0.840	0.004	−0.089	−0.076	0.008	0.012	−0.066	0.000	−0.101	−0.010	0.007
			0.000	0.000	0.840	−0.013	0.002	0.077	0.012	0.000	0.066	−0.025	0.002	0.011
			0.000	0.000	−0.840	−0.133	−0.004	−0.059	0.011	0.000	−0.066	−0.144	−0.004	0.007
			0.840	0.001	0.000	−0.870	0.021	0.049	−0.821	0.000	0.000	−0.050	0.021	0.049
			−0.840	−0.001	0.000	0.855	0.020	−0.007	0.860	0.000	0.000	−0.005	0.020	−0.007
−0.51	0.00	0.48	0.001	−0.840	−0.004	−0.060	0.072	−0.001	−0.012	0.066	0.000	−0.049	0.006	−0.001
			−0.001	0.840	0.004	−0.099	−0.072	−0.002	−0.011	−0.066	0.000	−0.088	−0.006	−0.003
			0.000	0.000	0.840	−0.094	−0.003	0.063	−0.011	0.000	0.066	−0.083	−0.003	−0.003
			0.000	0.000	−0.840	−0.074	−0.001	−0.068	−0.012	0.000	−0.066	−0.063	−0.001	−0.002
			0.840	0.001	0.000	−0.862	0.015	−0.043	−0.860	0.000	0.000	−0.002	0.015	−0.043
			−0.840	−0.001	0.000	0.840	0.001	0.038	0.821	0.000	0.000	0.019	0.001	0.038
0.51	0.00	1.52	−0.001	−0.840	−0.004	0.020	0.852	0.073	0.001	0.840	−0.004	0.019	0.012	0.077
			0.001	0.840	0.004	−0.068	−0.848	−0.050	0.000	−0.840	0.004	−0.068	−0.008	−0.054
			−0.001	0.000	0.840	0.021	0.006	0.863	0.001	0.000	0.840	0.020	0.006	0.023
			0.001	0.000	−0.840	−0.020	0.017	−0.834	−0.001	0.000	−0.840	−0.019	0.017	0.006
			0.840	−0.001	0.001	−0.846	0.097	0.013	−0.840	0.001	0.001	−0.006	0.097	0.012
			−0.840	0.001	−0.001	0.859	−0.020	0.024	0.840	−0.001	−0.001	0.019	−0.020	0.025
0.51	0.00	−2.48	0.001	−0.840	−0.004	0.030	0.486	−0.036	0.009	0.498	−0.002	0.022	−0.012	−0.034
			−0.001	0.840	0.004	−0.086	−0.490	0.013	0.010	−0.498	0.002	−0.096	0.008	0.011
			−0.002	0.000	0.840	0.035	0.014	0.465	0.011	0.000	0.498	0.024	0.014	−0.033
			0.002	0.000	−0.840	−0.045	−0.008	−0.446	0.008	0.000	−0.498	−0.053	−0.008	0.053
			0.840	0.001	0.002	−0.785	0.027	0.003	−0.824	0.000	0.001	0.040	0.027	0.002
			−0.840	−0.001	−0.002	0.781	−0.021	−0.029	0.856	0.000	−0.001	−0.075	−0.022	−0.027
1.49	0.00	−1.52	0.001	−0.840	−0.004	0.133	0.078	0.000	0.011	0.079	0.000	0.122	−0.001	0.001
			−0.001	0.840	0.004	0.008	−0.065	0.007	0.012	−0.079	0.000	−0.004	0.013	0.006
			−0.001	0.000	0.840	0.098	0.018	0.066	0.013	0.000	0.079	0.086	0.018	−0.013
			0.001	0.000	−0.840	−0.005	0.000	−0.073	0.010	0.000	−0.079	−0.016	0.000	0.006
			0.840	0.001	0.001	−0.758	0.006	0.070	−0.821	0.000	0.000	0.063	0.006	0.069
			−0.840	−0.001	−0.001	0.781	0.012	0.023	0.860	0.000	0.000	−0.079	0.012	0.023
1.49	0.00	0.48	0.000	−0.840	−0.004	0.115	0.318	0.016	0.011	0.292	−0.001	0.104	0.026	0.018
			0.000	0.840	0.004	0.002	−0.300	0.012	0.011	−0.292	0.001	−0.009	−0.008	0.011
			−0.001	0.000	0.840	0.127	0.016	0.288	0.012	0.000	0.292	0.115	0.016	−0.004
			0.001	0.000	−0.840	−0.001	0.007	−0.282	0.010	0.000	−0.292	−0.010	0.007	0.010
			0.840	0.000	0.001	−0.762	0.039	0.041	−0.822	0.000	0.000	0.060	0.039	0.041
			−0.840	0.000	−0.001	0.780	−0.008	0.027	0.858	0.000	0.000	−0.079	−0.008	0.028
1.49	0.00	2.48	0.000	−0.840	−0.004	0.037	0.755	0.051	0.004	0.778	−0.004	0.033	−0.023	0.055
			0.000	0.840	0.004	0.008	−0.740	−0.058	0.005	−0.778	0.004	0.004	0.038	−0.062
			−0.002	0.001	0.840	0.034	0.019	0.722	0.006	−0.001	0.778	0.028	0.020	−0.056
			0.002	−0.001	−0.840	−0.057	0.049	−0.704	0.002	0.001	−0.778	−0.060	0.048	0.074
			0.840	0.000	0.002	−0.778	0.034	−0.012	−0.833	0.000	0.002	0.054	0.035	−0.014
			−0.840	0.000	−0.002	0.788	−0.015	−0.014	0.847	0.000	−0.002	−0.060	−0.016	−0.012

in the least squares fit and weighted R factor (χ^2 64, $R_w = 15.5\%$) compared to those found for the original model (χ^2 76, $R_w = 17.0\%$). The poor R factor is due to the difficulty in measuring the weak intensities, which in turn confines the model to a simple Cu^{2+} spherical free ion form factor. The comparative insensitivity to moment direction provided by the least squares fit to the unpolarized neutron data serves to emphasize the superior nature of the polarimetry method, particularly when the magnetic scattering is weak and the moments are not confined to a single direction. The re-analysed moment component along [010] is 0.273(6) μ_B and the root mean square moment is 0.27(1) μ_B, which may be compared with the value quoted in the original paper of 0.30(2) μ_B.

References

Blume M 1963 *Phys. Rev.* **130** 1670
Brown P J, Nunez V, Tasset F, Forsyth J B and Radhakrishna P 1990 *J. Phys.: Condens. Matter* **2** 9409
Forsyth J B, Brown P J and Wanklyn B M 1988 *J. Phys. C: Solid State Phys.* **21** 2917
Tasset F 1989 *Physica* B **156–157** 627
Wanklyn B M and Garrard B J 1983 *J. Mater. Sci. Lett.* **2** 285
Yablonskii D 1990 *Physica* C **171** 454
Yang B X, Thurston T R, Tranquada J M and Shirane G 1989 *Phys. Rev.* B **39** 4343
Yang B X, Tranquada J M and Shirane G 1988 *Phys. Rev.* B **38** 174